Available online at www.sciencedirect.com
ScienceDirect
Trans. Nonferrous Met. Soc. China 33(2023) 3514−3528
Transactions of Nonferrous Metals Society of China
www.tnmsc.cn

Selective extraction of zinc from high iron-bearing zinc calcine by reduction and magnetization roasting

Tian-fu ZHANG, Jun-wei HAN, Sen LIU, Wei LIU, Chen LI, Fen JIAO, Wen-qing QIN

School of Minerals Processing and Bioengineering, Central South University, Changsha 410083, China

Received 19 May 2023; accepted 24 September 2023

Abstract: A novel process that combined reduction roasting with magnetization roasting was developed to intensify the decomposition of zinc ferrite for the selective extraction of zinc from high iron-bearing zinc calcine. The decomposition mechanism of zinc ferrite was investigated in detail by thermodynamics analysis and roasting experiments. The results indicated that 94.65% of the zinc ferrite was decomposed into zinc oxide and ferrous oxide under the optimal reduction roasting conditions of 8 vol.% CO, 750 °C, 50 vol.% CO/(CO+CO_2), and 90 min. The generated ferrous oxide was further converted to ferriferrous oxide by magnetization roasting under an air atmosphere at 450 °C for 30 min. After that, 93.62% of zinc contained in the calcine could be selectively extracted by low acid leaching, whereas more than 90% of iron was concentrated in the leaching slag in the form of magnetite, which could be recovered by the subsequent magnetic separation.

Key words: zinc ferrite; zinc calcine; reduction roasting; magnetization roasting; acid leaching

1 Introduction

Zinc is an important metal, which is widely applied in the alloys, battery, textile, and electroplating industry [1,2]. According to the statistics [3], the zinc production capacity of China reached 6.51×10^6 t in 2020, and about 80% of the metal zinc is primarily produced from zinc sulfide concentrates through the conventional hydrometallurgical process, which includes oxidative roasting, acid leaching, purification, and electrowinning steps [4,5]. In the oxidative roasting step, the iron impurity contained in the marmatite concentrates has a great potential to react with zinc oxide to generate zinc ferrite. Zinc ferrite is structurally stable and can hardly be dissolved by the conventional acid leaching process, as a result, large amounts of hazardous zinc-rich slag containing 16−28 wt.% Zn, 20−40 wt.% Fe, 0.5−1.5 wt.% Cu, and 2−12 wt.% Pb was produced [6−11].

To recover zinc from the hazardous zinc leaching slag, numerous methods have been developed, including the pyrometallurgical process, hydrometallurgical process, or their combination [12−14]. For the pyrometallurgical process, Ausmelt process [15] and Walze process [16,17] are most commonly applied in industry. Through the above processes, the zinc in the slag could be recycled with a high zinc recovery rate, and only little stable slag was produced. However, these processes are generally conducted at high temperatures, which consume huge energy. To avoid the above problems, a variety of hydrometallurgical processes including hot acid leaching [18,19] and hydrochloric acid leaching [20,21] were developed. By the hot acid leaching, the zinc contained in the slag can be completely extracted, whereas more than 80% of iron was also dissolved into leachate. To obtain high-quality zinc, the iron in the leachate has to be removed before electrowinning of zinc by the iron precipitation process [22,23]. Although the

Corresponding author: Wei LIU, Tel: +86-13787007421, E-mail: liuweipp1@126.com
DOI: 10.1016/S1003-6326(23)66351-4

iron in the leachate could be efficiently removed by the jarosite, goethite, and hematite processes [24−26], abundant hazardous iron slags were generated, which posed a great threat to the ecosystem. Hydrochloric acid leaching has also widely been studied on the laboratory scale recently, but these processes have never found application in the industry since the leachate cannot directly return to the existing electrowinning process.

Considering the weakness of conventional pyrometallurgical and hydrometallurgical processes, some scholars have recently focused on the combination of the above processes for the recycling of zinc or iron from high iron-bearing zinc calcine (IZ), such as reduction roasting−alkaline leaching [27], transformation roasting [28,29], sulfation roasting−water leaching [7,14], and selective reduction roasting [13,30,31]. The common characteristics of these technologies are to convert zinc ferrite into soluble zinc, and then facilitate the extraction of zinc by water leaching or low acid leaching. Although these novel processes have promising potential for energy conservation and pollution reduction, there are still many problems that need to be solved before industrial applications. Among these technologies, selective reduction roasting is one of the most interesting and has a great prospect in industrialization application. This process is to decompose the zinc ferrite in IZ to magnetite and zinc oxide by utilizing the waste heat in the calcine. Thereafter, zinc and iron can be selectively separated by the conventional acid leaching process, whereas iron and silver are concentrated in the leaching slag, which could be comprehensively recovered by magnetic separation and flotation, respectively. Despite the great progress obtained in recent years [32−34], two key issues presented in this technology including the complete decomposition of zinc ferrite and the controlling of the over-reduction of magnetite cannot be properly achieved simultaneously, especially in industry. This is attributed to the fact that zinc ferrite is a stable spinel structure, and the complete decomposition of which needs strong reducing conditions. However, magnetite is relatively unstable and thus the magnetite was inevitably over-reduced to wustite. Therefore, although the informed reduction roasting technologies [31,32,35] can relatively improve the leaching rate of zinc, the leaching rate of iron also increases significantly.

In response to the contradiction between the complete decomposition of zinc ferrite and the controlling of the over-reduction of magnetite, in this study, a novel roasting process that includes reduction and magnetization roasting to selectively intensify the decomposition of zinc ferrite in the IZ was proposed. Reduction roasting was conducted in a strong reduction atmosphere at a relatively high temperature to completely decompose zinc ferrite into zinc oxide and wustite. Then, taking advantage of the wustite that can be rapidly converted into magnetite in a thermal oxidizing atmosphere [36], the wustite generated in the previous stage was effectively converted into magnetite by means of magnetization roasting in a weak oxidizing atmosphere at a lower temperature. In the present study, the decomposition behavior of zinc ferrite, and the magnetization behavior of wustite during the roasting process were investigated in detail based on thermodynamic analysis and laboratory experiments. Moreover, the acid-leaching behaviors of the roasted products were also studied intensely. The generation of hazardous $ZnFe_2O_4$ slag can effectively be reduced, and an alternative process for the clean and efficient utilization of IZ was provided.

2 Experimental

2.1 Materials

The IZ used in this study was provided by a zinc smelter in Inner Mongolia, China. The zinc calcine was dried at 100 ℃ for 24 h, ground, and sieved to 80% below 74 μm for subsequent analysis tests and experiments. The chemical composition of zinc calcine was analyzed by X-ray fluorescence spectroscopy (XRF, S4 Pioneer, Bruker), and the results of which are shown in Table 1. The mineralogical structure of zinc calcine was characterized by X-ray diffraction analysis (XRD, D/Max 2500, Rigaku), and the results are presented in Fig. 1. Table 1 shows that the iron content in the zinc calcine reached 14.31 wt.%, indicating that the calcine is a typical IZ. Hence, in the conventional acid leaching process, a considerable amount of hazardous zinc leaching slag was generally produced. Figure 1 depicts that the zinc calcine is mainly composed of zinc oxide (ZnO), zinc silicate (Zn_2SiO_4), zinc ferrite ($ZnFe_2O_4$), and magnetite

Table 1 XRF analysis result of high-iron bearing zinc calcine (wt.%)

Zn	Fe	Pb	Cu	O
55.47	14.31	1.43	0.47	21.75
S	Si	Cd	Ca	others
2.71	1.46	0.21	0.78	1.42

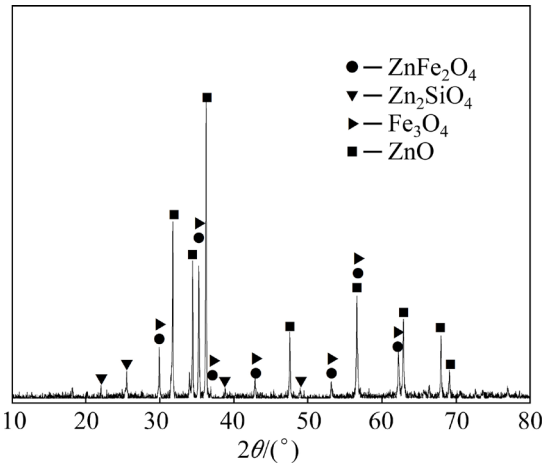

Fig. 1 XRD pattern of high iron-bearing zinc calcine

(Fe_3O_4). The phase compositions of zinc were quantified by selection dissolution of each zinc phase combined with inductively coupled plasma analysis (ICP-OES, PS-6, Baird), and the results are listed in Table 2. It can be seen that the quantity of $ZnFe_2O_4$ and ZnS in the zinc calcine reached 7.54 wt.% and 2.91 wt.%, respectively; therefore, the zinc in the calcine can hardly be completely leached.

In addition, carbon monoxide (CO, 99.9%) was used as a reducing gas to decompose zinc ferrite, carbon dioxide (CO_2, 99.9%) was applied to adjust the reduction intensity, and nitrogen (N_2, 99.9%) was used as a supplementary or protective gas during reduction roasting. At magnetization roasting stage, oxygen (O_2, 99.9%), N_2 and air were used to magnetize wustite. Sulfuric acid of the chemical grade was used as a lixiviant. In addition, zinc oxide and ferric oxide of analytical grade were used to investigate the zinc ferrite formation mechanism. Deionized water with a resistivity of 18 MΩ·cm was used throughout all leaching experiments.

2.2 Experimental procedure

The reduction and magnetization roasting experiments were conducted in a tube furnace (OTF, 1200X-S, Kejin). The schematic diagrams are shown in Fig. 2. For each roasting test, 50 g of prepared zinc calcine was put into the alundum boat (120 mm × 60 mm), which was taken into the tube furnace, and then heated to 750 °C in N_2 atmosphere. After that, a gas mixture containing a certain volume proportion of CO, CO_2, and N_2 was pumped into the tube furnace with a flow rate of 1000 mL/min until the roasting was finished. Then, the mixture gas was replaced by N_2 and cooled the sample to the magnetization temperature in the furnace. Whereafter, a gas mixed with O_2 and N_2 with a flow rate of 600 mL/min was pumped into the tube until the end of magnetization roasting. Finally, the roasted sample was taken out, weighed, and kept in the closed vessel for analysis and the following experiments. The zinc ferrite generation experiments were also conducted in the above tube furnace. Before roasting, zinc oxide and ferric oxide were homogenized with a molar ratio of 1:1, and ground in a planetary muller with a speed of 2000 r/min for 10 h. For each roasting test, 30 g of the above prepared sample was roasted in the tube in the air atmosphere. After the roasting was finished, the sample was cooled to room temperature and saved for subsequent analysis.

The leaching experiments were conducted in a 500 mL three-necked flat-bottomed flask, which

Table 2 Chemical phase analysis results of zinc in different samples

Phase	Unroasted sample		Magnetization roasted sample		Leaching slag	
	Mass fraction/%	Percentage/%	Mass fraction/%	Percentage/%	Mass fraction/%	Percentage/%
Oxide	42.68	78.37	51.61	93.62	–	–
Sulfate	1.33	2.44	–	–	–	–
Sulfide	2.91	5.34	2.27	4.12	9.57	66.87
Ferrite	7.54	13.85	1.24	2.25	4.74	33.13
Total	54.46	100.00	55.12	100	14.31	100

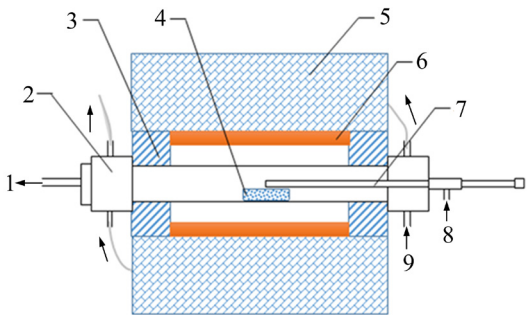

Fig. 2 Schematic diagram of tube furnace: 1−Escape pipe; 2−Cool system; 3−Asbestos board; 4−Porcelain boat; 5−Fireclay brick; 6−Heating zone; 7−Thermocouple; 8−Admitting pipe; 9−Water inlet

was equipped with a mechanical stirrer. For each leaching test, 30 g of the roasted zinc calcine was leached under the following conditions: 90 g/L of sulfuric acid, 10 mL/g of liquid-to-solid ratio, 30 min, and 25 °C. At the end of the leaching experiments, the leachate was separated from the slag by vacuum filtration. The volume of the leachate was measured by a graduated cylinder, and the concentrations of iron and zinc were analyzed by ICP. The leaching slag was dried, weighed, and kept in a closed vessel for subsequent analysis.

2.3 Analytical methods and instruments

The chemical compositions of all powder samples were detected by X-ray fluorescence spectroscopy (XRF, S4 Pioneer, Bruker), and the concentration of all leachate was analyzed by inductively coupled plasma analysis (ICP-OES, PS-6, Baird). The crystalline of the roasted samples was characterized by X-ray powder diffraction (XRD, D/Max 2500, Rigaku). The magnetism of samples was measured with a vibration sample magnetometer (VSM, BHV−50HTI). The soluble zinc rate (R) is calculated as

$$R=\frac{\Sigma\beta_i}{T_\alpha}\times 100\% \quad (1)$$

where $\Sigma\beta_i$ is the content of zinc distributed in soluble zinc (including ZnO, $ZnSO_4$, Zn_2SiO_4, and Zn), which could be obtained by the chemical analysis method in our previous study [32]; T_α is the total content of zinc.

The zinc ferrite generation rate (φ) and decomposition rate (χ) are calculated as follows:

$$\varphi=\frac{\theta}{\alpha}\times 100\% \quad (2)$$

$$\chi=\left(1-\frac{\gamma_2}{\gamma_1}\right)\times 100\% \quad (3)$$

where α is the total zinc content in the roasted sample; θ is the content of zinc distributed in zinc ferrite after roasting, which could be obtained by the chemical analysis method [32]; γ_1 and γ_2 are the zinc contents distributed in zinc ferrite before and after roasting, respectively.

The zinc and iron extraction rates are calculated by the following formula:

$$\varepsilon=\frac{c_i V_i}{m_1 \eta_i}\times 100\% \quad (4)$$

where ε is the extraction rate of zinc or iron, m_1 is the mass of samples, V_i is the volume of leachate, η_i is the content of zinc or iron in the samples, and c_i represents the concentration of zinc or iron in the leachate.

3 Results and discussion

3.1 Thermodynamic analysis

According to the phase composition of the IZ in this study, the reactions that probably occur at the reduction and magnetization roasting stage are listed as follows:

$ZnFe_2O_4+1/3CO(g)=ZnO+2/3Fe_3O_4+1/3CO_2$ (5)

$ZnFe_2O_4+CO=ZnO+2FeO+CO_2$ (6)

$ZnO+CO=Zn+CO_2$ (7)

$Fe_3O_4+CO=3FeO+CO_2$ (8)

$Fe_3O_4+4CO=3Fe+4CO_2$ (9)

$FeO+CO=Fe+CO_2$ (10)

$Fe+1/2O_2=FeO$ (11)

$Fe+2/3O_2=1/3Fe_3O_4$ (12)

$FeO+1/6O_2=1/3Fe_3O_4$ (13)

$FeO+1/4O_2=1/2Fe_2O_3$ (14)

$Fe_3O_4+1/4O_2=3/2Fe_2O_3$ (15)

$ZnO+Fe_2O_3=ZnFe_2O_4$ (16)

$ZnS+3/2O_2=ZnO+SO_2$ (17)

The standard Gibbs free energy changes (ΔG^Θ) for these reactions in the temperature range from 0 to 1200 °C were calculated by the Reactions module of FactSage 8.0 program, and the results are shown in Fig. 3. It can be found in Fig. 3(a) that the ΔG^Θ values for the decomposition of $ZnFe_2O_4$

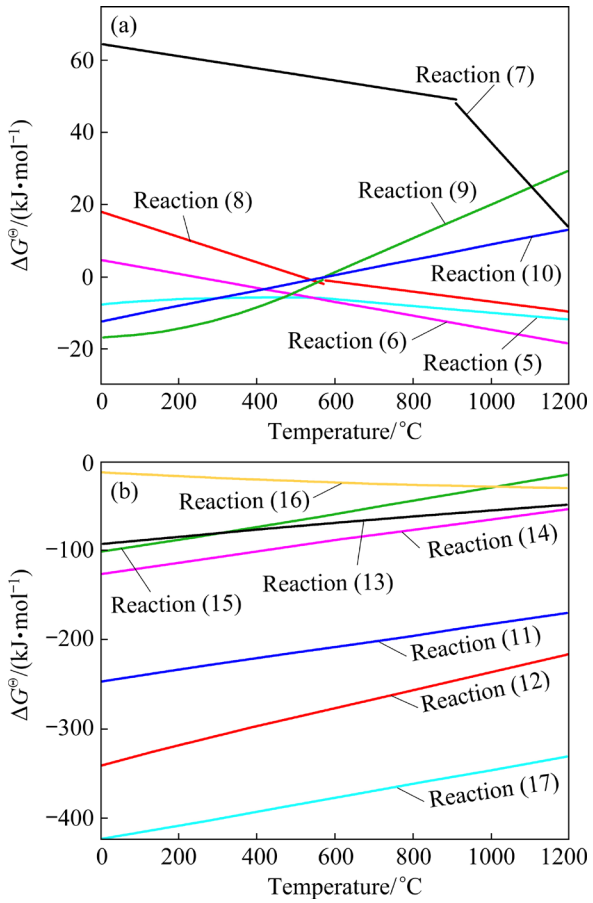

Fig. 3 Standard Gibbs free energy changes of reactions occurred possibly during reduction roasting (a) and magnetization roasting (b)

(Reaction (5)) are constantly negative at all temperatures in the investigated range, which decrease gradually with the increase in temperature, indicating that $ZnFe_2O_4$ can be decomposed into ZnO and Fe_3O_4, and the increase in temperature favors the above reduction process. However, the ΔG^{Θ} values of Reaction (6) decrease continuously with the temperature increasing from 100 to 1200 °C, and become more negative than those of Reaction (5) when the temperature increases up to 570 °C, which manifests that $ZnFe_2O_4$ has more potential to be reduced to ZnO and FeO. The ΔG^{Θ} variation tendency for the reduction of Fe_3O_4 to FeO (Reaction (8)) is similar to that for Reaction (6), and the ΔG^{Θ} also becomes negative at 570 °C, suggesting that the Fe_3O_4 generated during the decomposition of $ZnFe_2O_4$ might be further reduced to FeO. Therefore, the over-reduction of Fe_3O_4 can hardly be avoided. The ΔG^{Θ} of Reaction (7) is constantly positive in the investigated temperature range, manifesting that ZnO is thermodynamically stable. The ΔG^{Θ} values for Reactions (9) and (10) indicate that the generated Fe_3O_4 and FeO may be further reduced to Fe when the temperature is below 570 °C. The magnetization of FeO is another object of this study.

The ΔG^{Θ} values for the reactions that occur during magnetization roasting are presented in Fig. 3(b). It can be seen that the ΔG^{Θ} values of Reactions (11)−(15) are all negative in the investigated temperature range, which increase gradually with the increase in temperature. This indicates that decreasing temperature benefits the magnetization of Fe and FeO to Fe_3O_4, while the generated Fe_3O_4 may be further oxidized to Fe_2O_3. The ΔG^{Θ} values of Reaction (16) are negative in the temperature range from 0 to 1200 °C and decrease with increasing temperature, indicating that the Fe_2O_3 may continuously react with ZnO to generate $ZnFe_2O_4$, and decreasing magnetization temperature can inhibit the above process. Moreover, it can also be found that magnetization roasting is favorable to the oxidation of ZnS since the ΔG^{Θ} values for Reaction (17) are constantly negative. Therefore, to magnetize FeO to Fe_3O_4 and avoid the regeneration of $ZnFe_2O_4$, the magnetization roasting should be carried out at a relatively low temperature.

The equilibrium amounts of products for the decomposition reactions and magnetization reactions were calculated using the Equilibrium module of Outokumpu HSC Chemistry 9.0, and the results are shown in Fig. 4.

The effect of temperature in the range of 0−1000 °C on the decomposition behavior of $ZnFe_2O_4$ was investigated. According to the stoichiometric ratio of Reaction (6), both CO and $ZnFe_2O_4$ input amounts were fixed at 1 kmol, and the results are shown in Fig. 4(a). It indicates that increasing temperature can not only obviously promote the decomposition of $ZnFe_2O_4$ to ZnO and FeO, but also hinder the over-reduction of FeO to Fe. However, as the temperature increases to 1000 °C, the amount of $ZnFe_2O_4$ is still about 0.18 kmol, indicating that $ZnFe_2O_4$ can hardly be completely decomposed using the theoretical amount of CO. Since the content of $ZnFe_2O_4$ decreases slightly as the temperature increases above 750 °C, the effect of CO amount in the range of 0−3 kmol (per 1 kmol $ZnFe_2O_4$) on the equilibrium amounts of $ZnFe_2O_4$ decomposition products is presented in Fig. 4(b). The amount of

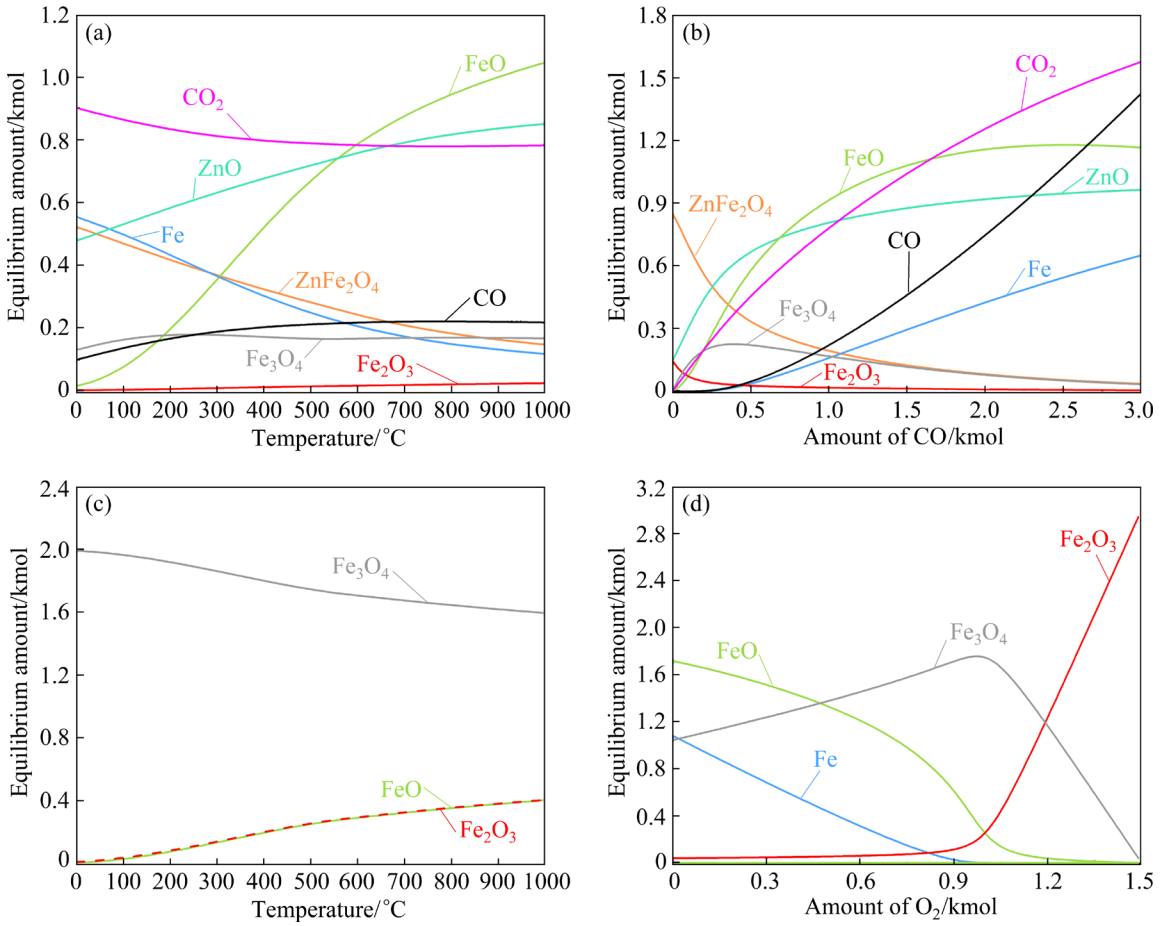

Fig. 4 Equilibrium compositions of iron-containing species during reduction roasting (a, b) and magnetization roasting (c, d): (a, c) Effect of temperature; (b) Effect of CO amount; (d) Effect of O_2 amount

$ZnFe_2O_4$ decreases sharply as the CO input amount increases from 0 to 2.5 kmol, and then, with further increase of CO amount, the value decreases slowly (about 0.03 kmol), while the amount of Fe increases dramatically. This manifests that the increase in CO input amount intensifies not only the decomposition of $ZnFe_2O_4$ but also the reduction of FeO to Fe. Additionally, it is also found that the CO and CO_2 amounts for the complete decomposition of $ZnFe_2O_4$ are about 1.43 and 1.57 kmol, respectively. Therefore, the proportion of CO during reduction roasting is required to be higher than 47.7%. While the amount of Fe_3O_4 increases rapidly with the CO input amount increasing from 0 to 0.2 kmol, thereafter, it decreases gradually, indicating that Fe_3O_4 is over-reduced to FeO. Above all, the complete decomposition of $ZnFe_2O_4$ could be achieved under a high CO proportion, but Fe_3O_4 is inevitably reduced to FeO.

Another object of this work is to magnetize the over-reduced soluble iron phase to Fe_3O_4. Thus, the effect of temperature on the equilibrium amounts of iron phase magnetization products was investigated, and the FeO and O_2 input amounts were fixed at 6 and 1 kmol, respectively. The results are shown in Fig. 4(c). It is observed from Fig. 4(c) that the amount of Fe_3O_4 decreases gradually with the temperature increasing from 0 to 1000 °C. On the contrary, the amounts of FeO and Fe_2O_3 increase slowly, demonstrating that the increase in temperature not only hinders the magnetization of FeO but also intensifies the generation of Fe_2O_3. However, low temperature will generally result in slow reaction speed, and thus, the magnetization temperature was chosen to be 500 °C. Figure 4(d) shows the effect of the O_2 input amount on the magnetization behavior of FeO at 500 °C, where the FeO input amount was fixed at 6 kmol. It is found that the increase in O_2 input amount significantly intensifies the magnetization of FeO to Fe_3O_4 when the O_2 input amount is lower than the theoretical amount (1 kmol), but too high O_2 input amount will

result in further oxidation of Fe_3O_4 to Fe_2O_3.

According to the above thermodynamic analysis, the complete decomposition of $ZnFe_2O_4$ and magnetization of FeO can be achieved by controlling the roasting temperature and atmosphere.

3.2 Formation mechanism of zinc ferrite

The previous thermodynamics analysis indicates that zinc ferrite may be regenerated during magnetization roasting. To achieve the selective magnetization of wustite, it is necessary to investigate the formation mechanism of zinc ferrite. The effect of magnetization roasting temperature on the formation of zinc ferrite was investigated when the roasting time was fixed at 60 min. The results are presented in Figs. 5(a) and (c). It can be seen from Fig. 5(a) that the zinc ferrite synthesis rate increases slowly and kept at a low level (about 2%) when the temperature is not above 500 °C. However, as the temperature is further increased, the synthesis rate increases dramatically and even reaches 83.4% at 650 °C. Additionally, the XRD analysis results in Fig. 5(c) also demonstrate that the zinc ferrite is not generated until the roasting temperature is increased above 500 °C, and this result is consistent with the conclusion of WANG et al [37]. Therefore, to avoid the regeneration of zinc ferrite, the magnetization temperature cannot be higher than 500 °C.

Roasting time is another key factor for the generation of zinc ferrite. The effect of roasting time on the formation of zinc ferrite was investigated in detail at the roasting temperature of 500 °C. The results are shown in Figs. 5(b) and (d). Figure 5(b) shows that the zinc ferrite synthesis rate increases from 0.78% to 1.85% as the roasting time is prolonged from 15 to 90 min, indicating that prolonging roasting time can also promote the formation of zinc ferrite, but the effect of which is weak and less than that of temperature, and the XRD analysis in Fig. 5(d) also demonstrates the above inference.

In conclusion, the regeneration rate of zinc ferrite can be controlled in a very small range during magnetization roasting by regulating the roasting temperature not higher than 500 °C, and time no longer than 60 min.

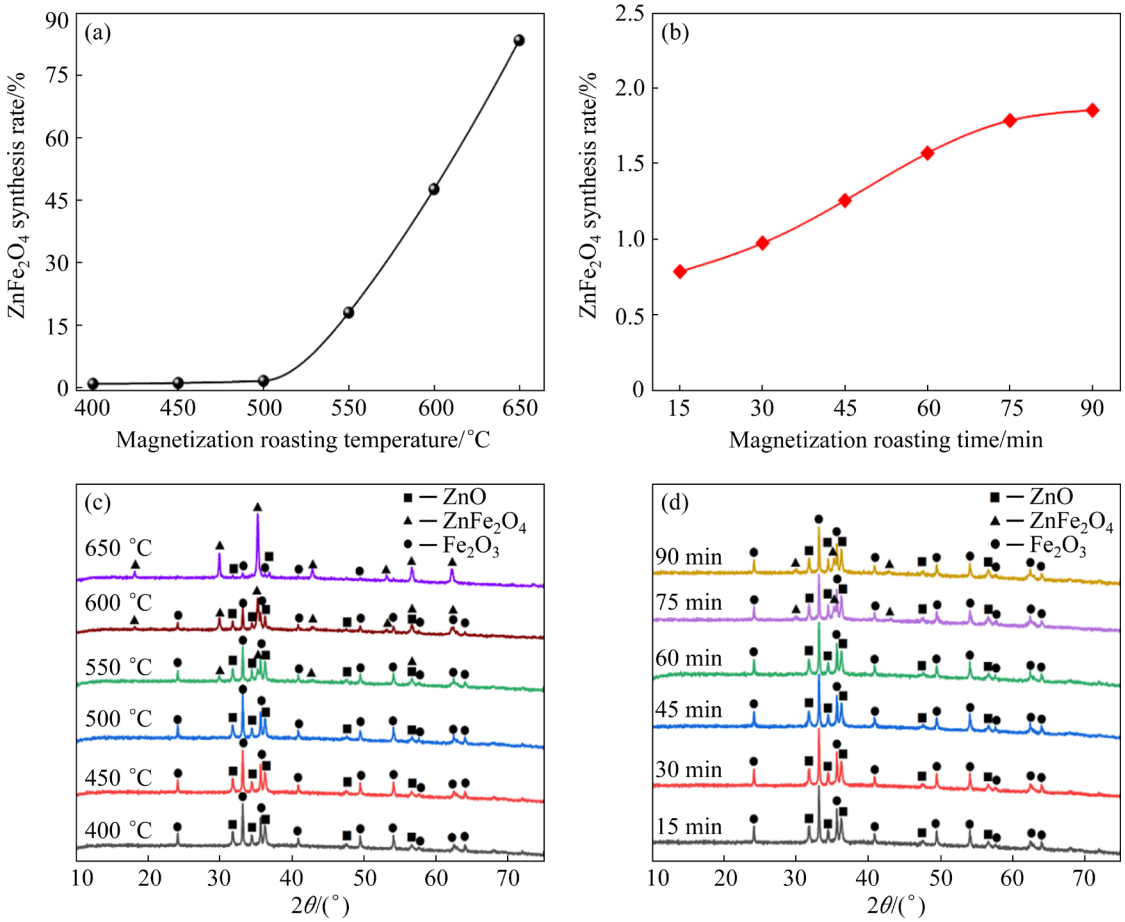

Fig. 5 Effect of magnetization roasting temperature (a, c) and time (b, d) on generation of zinc ferrite: (a, b) Zinc ferrite synthesis rate; (c, d) XRD patterns of roasted products

3.3 Reduction decomposition behavior of zinc ferrite

An ideal result for the complete decomposition of zinc ferrite was obtained from the thermodynamic analysis. However, it is also essential to conduct a series of experiments on the laboratory scale to prove the above conclusions. In this study, the main factors including CO concentration, temperature, CO/(CO+CO_2) volume fraction, and time on the reduction decomposition behavior of zinc ferrite were investigated in detail.

The effect of CO concentration on the reduction decomposition of zinc ferrite was investigated firstly at 750 °C for 120 min, and the results are shown in Figs. 6(a, b). Figure 6(a) indicated that both the zinc ferrite decomposition rate (χ) and soluble zinc rate (R) of roasted samples significantly increased from 70.16% and 88.41% to 95.89% and 94.55%, respectively, with the concentration of CO increasing from 4 vol.% to 8 vol.%. Thereafter, with further increase in CO concentration, the values gradually leveled off and remained nearly constant. These indicated that increasing CO concentration obviously facilitated the decomposition of zinc ferrite, and the majority of zinc ferrite could be decomposed with 8 vol.% CO. The XRD patterns of roasted samples in Fig. 6(b) indicated that zinc ferrite was decomposed completely when the CO concentration increased to 8 vol.%. Therefore, the optimized CO concentration was determined to be 8 vol.%.

Reduction roasting temperature plays a key role in the decomposition of zinc ferrite [38−40]. Hence, the effect of temperature on the decomposition behaviors of zinc ferrite was further investigated under the conditions of 8 vol.% of CO concentration and 120 min of roasting time. The results are presented in Figs. 6(c, d). Figure 6(c) showed that χ and R values increased significantly as the reduction roasting temperature was raised from 450 to 750 °C. However, the values did not increase substantially with a further increase in temperature. The increase in χ and R values is probably attributed to the decomposition of zinc ferrite being kinetically restricted. Increasing temperature accelerated the decomposition reaction rate of zinc ferrite. Figure 6(d) indicated that zinc ferrite in the calcine was reduced to zinc oxide completely at 750 °C. The increase in reduction temperature not only promoted the decomposition of zinc ferrite, but also facilitated the metallization of wustite. However, the iron oxides were over-reduced to metallic iron.

To avoid the generation of iron, CO_2 was used to regulate the reduction intensity. The effect of the CO/(CO+CO_2) volume fraction on the decomposition of zinc ferrite was studied at 8 vol.% CO. The results are presented in Figs. 6(e, f). It can be found from Fig. 6(e) that χ and R increased dramatically when the CO/(CO+CO_2) volume fraction increased from 33.4% to 50%, and the value of χ gradually leveled off, while the R decreased slightly, when the CO/(CO+CO_2) volume fraction exceeded 50%. The decrease of R may be attributed to the reduction of zinc sulfate to zinc sulfide. Hence, the optimal CO/(CO+CO_2) volume fraction was confirmed to be 50%. The XRD patterns of roasted samples are shown in Fig. 6(f). It was found that the metallic iron was not detected in all roasted samples, the diffraction peak intensity of zinc ferrite decreased sharply and its position (2θ=35.26°) had an obvious right shift (Fe_3O_4, 2θ=35.43°) when the CO/(CO+CO_2) volume fraction increased from 33.4% to 40%. Then, further increasing the CO/(CO+CO_2) volume fraction to 50%, the characteristic peaks of magnetite disappeared, while the peak intensity of wustite increased obviously. These variations indicated that the addition of CO_2 could hinder the over-reduction of wustite; hence, the zinc ferrite could be selectively decomposed into wustite and zinc oxide. Additionally, it was also observed that the peak intensity of zinc sulfide increased gradually with the CO/(CO+CO_2) volume fraction increasing from 50% to 66.7%, depicting that the soluble zinc sulfate was converted to zinc sulfide, hence resulting in the decrease of R in Fig. 6(e).

The effect of reduction roasting time on the decomposition of zinc ferrite was also investigated under the conditions of 750 °C, 8 vol.% CO, and 50 vol.% CO/(CO+CO_2). The results are presented in Figs. 6(g, h). Figure 6(g) showed that the variation of χ and R with the increase in reduction time was similar to that of CO/(CO+CO_2) volume fraction. Both set parameters increased sharply in the initial reduction period, which was attributed to the continuous decomposition of zinc ferrite to zinc oxide. However, since the reduction of zinc sulfide, the value of R decreased gradually with the reduction time prolonging from 90 to 150 min.

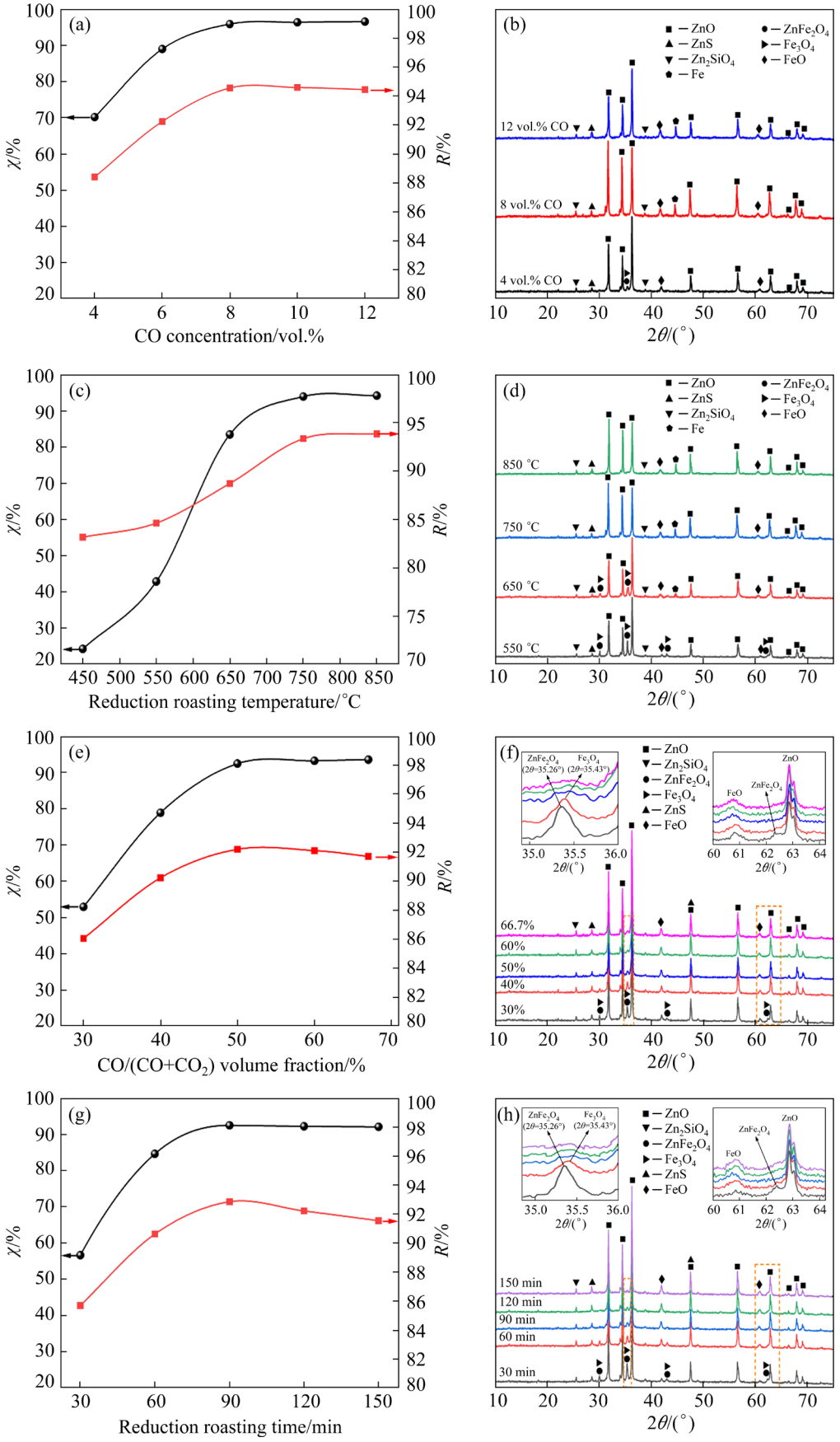

Fig. 6 Effect of reduction roasting conditions on decomposition of high iron-bearing zinc calcine: (a, b) Effect of CO concentration; (c, d) Effect of reduction roasting temperature; (e, f) Effect of $CO/(CO+CO_2)$ volume fraction; (g, h) Effect of reduction roasting time

The XRD patterns of roasted samples at different roasting time are shown in Fig. 6(h). The results indicated that the peaks of zinc ferrite and magnetite disappeared at 90 min, and the iron phase analysis results in Table 3 revealed that the iron in the reduced sample was mainly distributed in the form of wustite (70.65%) and magnetite (23.24%). The above variation manifested that most of the zinc ferrite was reduced to zinc oxide and wustite. Moreover, it was also found that the increase in reduction time promoted the generation of zinc sulfide since the peak intensity of zinc sulfide obviously increased with increasing the time from 90 to 150 min. Therefore, the optimal decomposition time was determined to be 90 min.

In conclusion, the optimal conditions for the decomposition of zinc ferrite during reduction roasting were established as follows: 8 vol.% CO, 750 °C, 50 vol.% $CO/(CO+CO_2)$, and 90 min. Under the above conditions, the zinc ferrite in the zinc calcine was selectively decomposed into zinc oxide and wustite, and the χ and R of the roasted sample reached 94.65% and 93.85%, respectively.

Table 3 Chemical phase analysis results of iron in sample after 90 min reduction roasting

Phase	Mass fraction/%	Percentage/%
Wustite	10.52	70.65
Magnetite	3.46	23.24
Zinc ferrite	0.78	5.24
Metallic iron	0.13	0.87
Total	14.89	100

3.4 Magnetization behavior of wustite

After reduction roasting, the zinc ferrite contained in the IZ was decomposed into zinc oxide and wustite. To realize the selective separation and recovery of zinc and iron in the subsequent processes, the soluble wustite generated during the reduction roasting stage must be converted to magnetite. The previous study in Sections 3.1 and 3.2 manifested that wustite can be selectively converted to magnetite and avoid the regeneration of zinc ferrite simultaneously by regulating the magnetization roasting conditions. Therefore, the effect of temperature, O_2 concentration, and time on the magnetization of wustite was detailly investigated. The results are shown in Fig. 7.

The effect of temperature on the magnetization of reduction product was investigated in air atmosphere (about 21 vol.% O_2) at roasting time of 15 min. The results are shown in Figs. 7(a, b). It can be found from Fig. 7(a) that the leaching rate of iron decreased dramatically, whereas that of zinc kept basically unchanged as the temperature increased from 400 to 450 °C, thereafter, both of them decreased slowly with the further increase in temperature. This may be attributed to the increase in temperature that intensified the conversion of wustite to magnetite, thus decreasing the leaching rate of iron; but high roasting temperature (above 450 °C) would promote the regeneration of zinc ferrite and then hinder the extraction of zinc. Moreover, the XRD patterns in Fig. 7(b) also proved that the wustite was completely converted into magnetite at 450 °C. It was also found that the zinc ferrite generated at 500 °C, and the peak intensity of which increased obviously with the increase of temperature. Therefore, the optimal temperature for the magnetization of wustite was confirmed to be 450 °C.

The O_2 concentration also has a significant effect on the magnetization of wustite. The effect of O_2 concentration on the magnetization of reduction product was investigated at 450 °C and 15 min. The results are presented in Figs. 7(c, d). Figure 7(c) showed that the zinc leaching rate slowly increased with the concentration of O_2 increasing from 5 vol.% to 21 vol.% (air) and then decreased gradually as the O_2 concentration further increased. The increase in zinc leaching rate is probably ascribed to the oxidation of zinc sulfide to zinc sulfate. The leaching rate of iron first decreased sharply and then gradually slowed down, indicating that the increase in O_2 concentration contributed to the magnetization of wustite when O_2 concentration was below 21 vol.%; whereas, with further increasing O_2 concentration, the generated magnetite was probably further oxidized to ferric oxide, which in turn intensified the formation of zinc ferrite. However, since the formation of zinc ferrite was kinetics (temperature) restricted, resulting in the slow generation speed of zinc ferrite at 450 °C, both the leaching rates of zinc and iron just slowly decreased when O_2 concentration increased above 21 vol.%. Figure 7(d) showed that the peak intensity of zinc sulfide decreased gradually with the increase of O_2 concentration. The peak of wustite disappeared at 21 vol.% of O_2 concentration

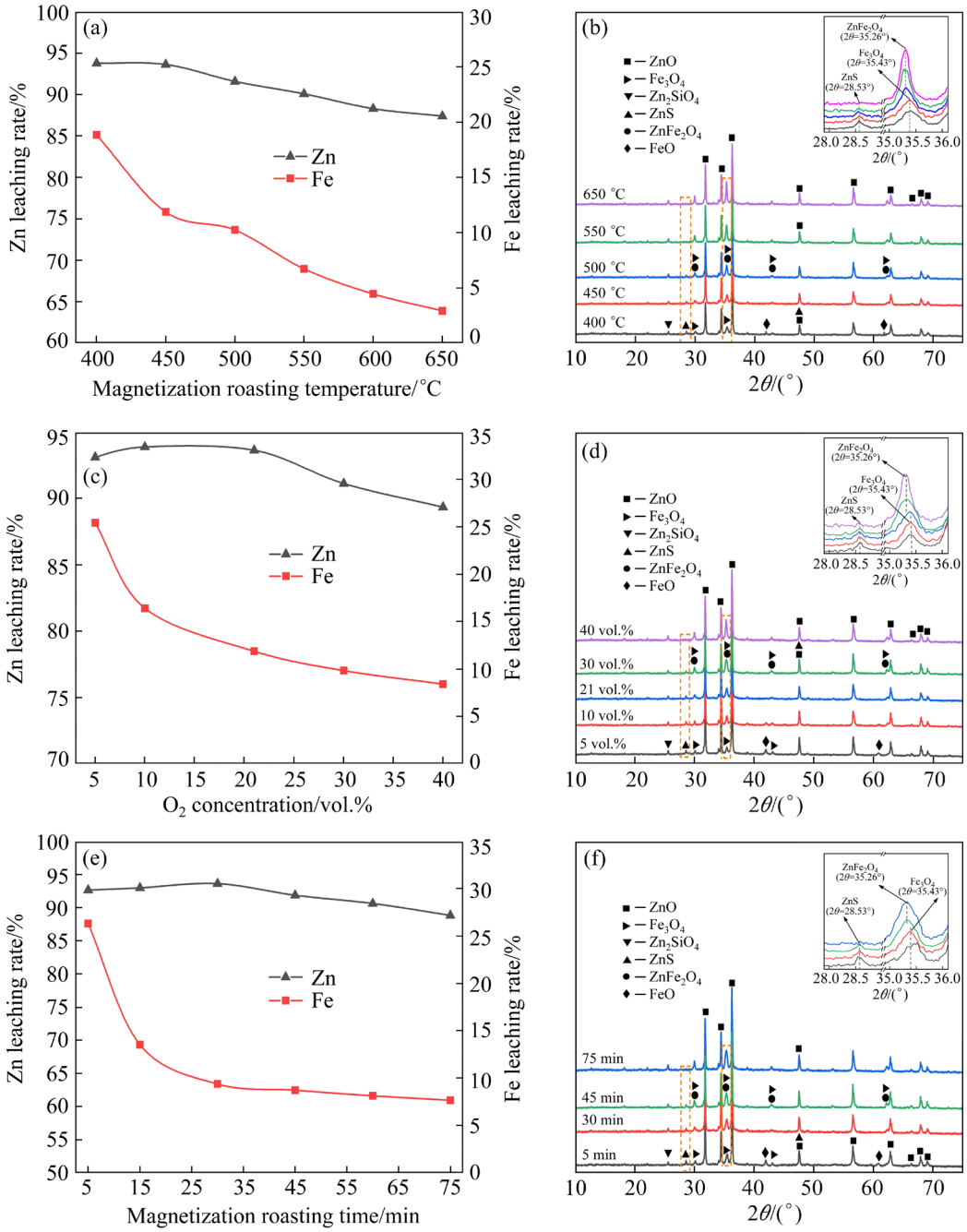

Fig. 7 Effect of roasting conditions on magnetization behavior of wustite: (a, b) Effect of magnetization roasting temperature; (c, d) Effect of O_2 concentration; (e, f) Effect of magnetization roasting time

and the peak intensity of magnetite obviously increased. Then, with further increasing the O_2 concentration, the peak position of magnetite (2θ= 35.43°) gradually left-shifted ($ZnFe_2O_4$, 2θ=35.26°). These results confirmed the inference that increasing the O_2 concentration resulted in the oxidation of zinc sulfide and the regeneration of zinc ferrite. Therefore, air (21 vol.% O_2) was used as the magnetization gas.

The effect of roasting time on the magnetization of wustite was also investigated in the air atmosphere at 450 °C. The results are shown in Figs. 7(e, f). Figure 7(e) showed that prolonging the roasting time favored the selective leaching of zinc, since the zinc leaching rate slightly increased from 92.65% to 93.62%, while the iron leaching rate dramatically decreased from 26.32% to 9.37% as the duration time increased from 5 to 30 min. However, both the leaching rates of zinc and iron gradually decreased as the roasting time further increased (above 30 min), which was approximately attributed to the regeneration of zinc ferrite.

Figure 7(f) showed that the characteristics peak of wustite disappeared and the peak intensity of magnetite increased significantly when the magnetization roasting time increased from 5 to 30 min, indicating that the wustite was completely converted into magnetite. However, as the magnetization roasting time further increased (above 30 min), the zinc ferrite generated gradually. In addition, Table 2 demonstrated that the zinc distributed in the zinc ferrite and zinc sulfide contained in the magnetization roasted sample were decreased to 1.24% and 2.27%, respectively, depicting that the selective decomposition of zinc ferrite was achieved.

In summary, the optimal conditions for the magnetization roasting were under an air atmosphere at 450 °C for 30 min. Under the above conditions, the leaching rate of zinc reached 93.62%, whereas that of iron was only 9.37%.

The magnetic hysteresis loops of the zinc calcine before roasting (Curve a), after reduction roasting (Curve b), and after magnetization roasting (Curve c) were investigated by the VSM. The results are presented in Fig. 8. It could be found that the saturation magnetization of the zinc calcine increased from 2.26 to 4.45 to 15.88 A·m^2/kg after the reduction roasting and magnetization roasting under their optimal conditions, respectively, which further confirmed that the zinc ferrite contained in the zinc calcine was selectively decomposed into magnetite after reduction and magnetization roasting.

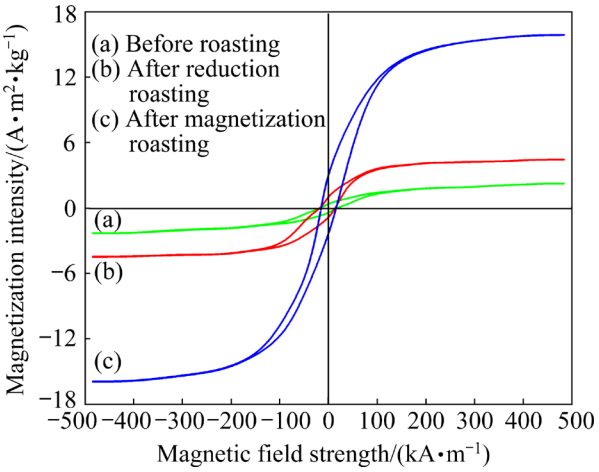

Fig. 8 Magnetic hysteresis loops of zinc calcines

According to the above analysis, the selective decomposition mechanism of zinc ferrite is depicted in Fig. 9. It can be summarized as follows: First, the zinc ferrite in the calcine was completely reduced and decomposed into FeO and ZnO with high CO proportion at a higher temperature. In the second stage, the FeO generated in the first stage was selectively magnetized into Fe_3O_4 by gas−solid reaction with O_2 in air at a lower temperature. Due to the low magnetization temperature and the limitation of kinetic reaction rate, zinc ferrite is difficult to generate in the second stage. Therefore, the selective reduction of zinc ferrite could be achieved through reduction and magnetization roasting.

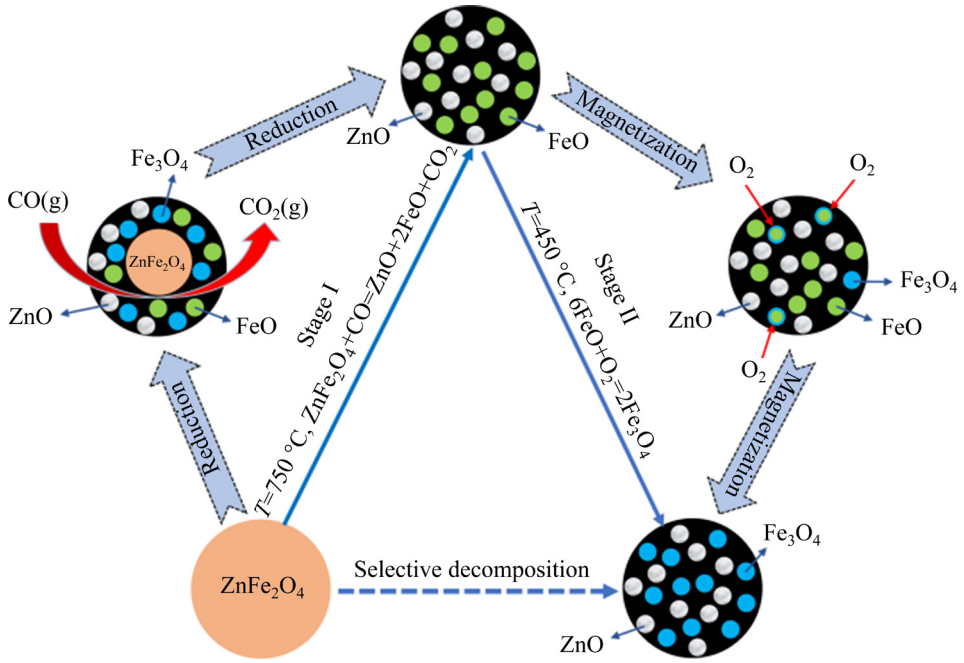

Fig. 9 Selective decomposition mechanism of zinc ferrite

3.5 Composition of leaching slag

The main chemical compositions of the acid leaching slag for the roasted sample and unroasted sample are presented in Table 4. It can be found that after the reduction and magnetization roasting, the contents of zinc and copper in the leaching slag decreased from 25.44% and 0.51% to 14.72% and 0.18%, respectively, while the content of iron increased from 38.23% to 47.96%. These indicated that the above roasting process not only promoted the selective extraction of zinc, but also intensified the leaching of copper. To clarify the phase composition, the leaching slag of the roasted sample was further subjected to XRD analysis, and the result is shown in Fig. 10. Figure 10 indicated that the main crystalline phases contained in the slag were magnetite, zinc sulfide, and zinc ferrite. Compared with those in Fig. 7(f), zinc oxide and zinc silicate were leached completely. The chemical phase analysis results (Table 2) indicate that the zinc in the leaching slag is mainly distributed in the form of zinc sulfide (9.57 wt.%) and zinc ferrite (4.74 wt.%), and thus the presence of unoxidized zinc sulfide and undecomposed zinc ferrite is the prime reason to hinder the leaching of zinc during the acid leaching process.

Table 4 Quantitative chemical phase analysis results of main elements in leaching slag (wt.%)

Sample	Zn	Fe	Cu	Pb	Co
Unroasted	25.44	38.23	0.51	3.54	0.05
Roasted	14.72	47.96	0.18	4.32	0.06

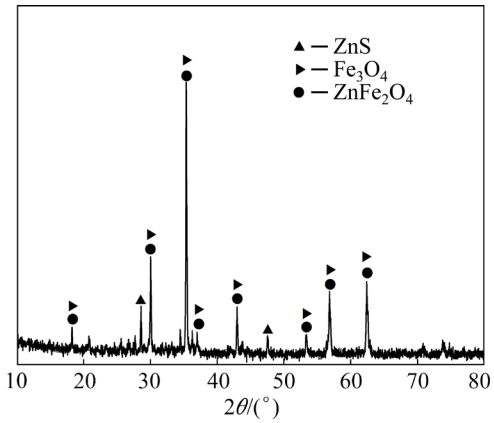

Fig. 10 XRD pattern of leaching slag

4 Conclusions

(1) Thermodynamic analysis shows that the over-reduction of magnetite is unavoidable at the reduction roasting stage. Increasing the reduction roasting temperature and CO amount could not only intensify the decomposition of zinc ferrite but also promote the formation of wustite. The generated wustite can be selectively converted to magnetite by regulating the magnetization temperature and input O_2 amount.

(2) Zinc ferrite generation experimental results indicate that by controlling the roasting temperature not higher than 500 °C and time no longer than 60 min, the regeneration of zinc ferrite during the magnetization roasting stage can be effectively restrained.

(3) Increasing the reduction roasting parameters of CO concentration, temperature, $CO/(CO+CO_2)$ volume fraction and time significantly intensifies the decomposition of zinc ferrite to zinc oxide and wustite. However, when these parameters exceed their optimal levels, the zinc sulfate will be reduced to zinc sulfide. Under the optimal conditions of 8 vol.% CO, 750 °C, 50 vol.% $CO/(CO+CO_2)$, and 90 min, the zinc ferrite decomposition rate and soluble zinc rate of the roasted sample reached 94.65% and 93.85%, respectively.

(4) The wustite generated at the reduction roasting stage was selectively converted to magnetite by magnetization roasting in air atmosphere at 450 °C for 30 min. Then, 93.62% of zinc contained in the zinc calcine was selectively extracted by the low acid leaching. More than 90% of the iron was concentrated into leaching slag in the form of magnetite, which could be recovered by a conventional magnetic separation process.

Acknowledgments

The authors gratefully acknowledge the financial supports from the National Natural Science Foundation of China (Nos. 52174269, 51874356), the National Key R&D Program of China (Nos. 2019YFC1907301, 2020YFC1909203, 2018YFC1900301, 2018YFC1902500), the Landmark Innovation Demonstration Project of Hunan Province, China (No. 2019XK2304), the Innovation Driven Project of Central South University, China (No. 2020CX038), the Natural Science Foundation of Hunan Province, China (No. 2019JJ50805), and the Scientific Research Starting Foundation of Central South University, China (No. 218041).

References

[1] JHA M K, KUMAR V, SINGH R J. Review of hydrometallurgical recovery of zinc from industrial wastes [J]. Resources, Conservation and Recycling, 2001, 33(1): 1−22.

[2] VENEZUELA J, DARGUSCH M S. The influence of alloying and fabrication techniques on the mechanical properties, biodegradability and biocompatibility of zinc: A comprehensive review [J]. Acta Biomaterialia, 2019, 87: 1−40.

[3] WANG Jie, ZHANG Ying-yi, CUI Kun-kun, FU Tao, GAO Jian-jun, ALGARNI T S. Pyrometallurgical recovery of zinc and valuable metals from electric arc furnace dust—A review [J]. Journal of Cleaner Production, 2021, 298: 126788.

[4] CHEN T T, DUTRIZAC J E. Mineralogical changes occurring during the fluid-bed roasting of zinc sulfide concentrates [J]. JOM, 2004, 56(12): 46−51.

[5] BOYANOV B, PELTEKOV A, PETKOVA V. Thermal behavior of zinc sulfide concentrates with different iron content at oxidative roasting [J]. Thermochimica Acta, 2014, 586: 9−16.

[6] LIN Hong-fu, WENG Wei, ZHONG Shui-ping, QIU Guan-zhou. Enhanced recovery of zinc and lead by slag composition optimization in rotary kiln [J]. Transactions of Nonferrous Metals Society of China, 2022, 32: 3110−3122.

[7] LI Yan-chun, LIU Hui, PENG Bing, MIN Xiao-bo, HU Min, PENG Ning, YUANG Ying-zheng, LEI Jie. Study on separating of zinc and iron from zinc leaching residues by roasting with ammonium sulphate [J]. Hydrometallurgy, 2015, 158: 42−48.

[8] PENG Ning, PENG Bing, CHAI Li-yuan, LIU Wei, YAN Huan, HOU Dong-ke. Decomposition of zinc ferrite in zinc leaching residue by reduction roasting [J]. Procedia Environmental Sciences, 2012, 16(4): 705−714.

[9] XU Da-mao, FU Rong-bing. The mechanistic insights into the leaching behaviors of potentially toxic elements from the indigenous zinc smelting slags under the slag dumping site scenario [J]. Journal of Hazardous Materials, 2022, 437: 129368.

[10] KASHYAP V, TAYLOR P. Extraction and recovery of zinc and indium from residue rich in zinc ferrite [J]. Minerals Engineering, 2022, 176: 107364.

[11] LI Yan-chun, ZHUO Shen-na, PENG Bing, MIN Xiao-bo, LIU Hui, KE Yong. Comprehensive recycling of zinc and iron from smelting waste containing zinc ferrite by oriented transformation with SO_2 [J]. Journal of Cleaner Production, 2020, 263: 121468.

[12] HAN Jun-wei, LIU Wei, QIN Wen-qing, PENG Bing, YANG Kang, ZHENG Yong-xing. Recovery of zinc and iron from high iron-bearing zinc calcine by selective reduction roasting [J]. Journal of Industrial & Engineering Chemistry, 2015, 22: 272−279.

[13] HAN Jun-wei, LIU Wei, QIN Wen-qing, YANG Kang, LUO Hong-lin. Innovative methodology for comprehensive utilization of high iron bearing zinc calcine [J]. Separation and Purification Technology, 2015, 154: 263−270.

[14] WANG Yi-zhuang, LIU Bing-bing, SUN Hu, HUANG Yan-fang, HANG Gui-hong. Selective extraction and recovery of tin from hazardous zinc-leaching residue by oxalic acid/sulfuric acid mixture leaching and hydrolytic precipitation [J]. Journal of Cleaner Production, 2022, 342: 130955.

[15] HOANG J, REUTER M A, MATUSEWICZ R. Top submerged lance direct zinc smelting [J]. Minerals Engineering, 2009, 22: 742−751.

[16] STEWART D, BARRON A R. Pyrometallurgical removal of zinc from basic oxygen steelmaking dust—A review of best available technology [J]. Resources, Conservation and Recycling, 2020, 157: 104746.

[17] ANTUANO N, CAMBRA J F, ARIAS P L. Development of a combined solid and liquid wastes treatment integrated into a high purity ZnO hydrometallurgical production process from Waelz oxide [J]. Hydrometallurgy, 2017, 173: 250−257.

[18] LI Xuan-hai, ZHANG Yan-juan, PAN Liu-ping, WEI Yan-song. Effect of mechanical activation on dissolution kinetics of neutral leach residue of zinc calcine in sulphuric acid [J]. Transactions of Nonferrous Metals Society of China, 2013, 23: 1512−1519.

[19] ZHANG Fan, WEI Chang, DENG Zhi-gan, LI Cun-xiong, LI Xing-bin. Reductive leaching of zinc and indium from industrial zinc ferrite particulates in sulphuric acid media [J]. Transactions of Nonferrous Metals Society of China, 2016, 26: 2495−2501.

[20] WANG Hong-jun, LIU Zhi-yong, LIU Zhi-hong, LI Yu-hu, LI Si-wei, ZHANG Wen-hai. Leaching of iron concentrate separated from kiln slag in zinc hydrometallurgy with hydrochloric acid and its mechanism [J]. Transactions of Nonferrous Metals Society of China, 2017, 27: 901−907.

[21] ZHANG Tian-fu, LIU Wei, HAN Jun-wei, WU Gui-tin, QIN Wen-qing. Selective separation of calcium from zinc-rich neutralization sludge by sulfidation roasting and HCl leaching [J]. Separation and Purification Technology, 2021, 259: 118064.

[22] HOEBER L, STEINLECHNER S. A comprehensive review of processing strategies for iron precipitation residues from zinc hydrometallurgy [J]. Cleaner Engineering and Technology, 2021, 4: 100214.

[23] HAN Hai-sheng, SUN Wei, HU Yue-hua, JIA Bao-liang, TANG Hong-hu. Anglesite and silver recovery from jarosite residues through roasting and sulfidization−flotation in zinc hydrometallurgy [J]. Journal of Hazardous Materials, 2014, 278: 49−54.

[24] SINGH V K, MANNA S, BISWAS J K. Recovery of residual metals from jarosite waste using chemical and biochemical processes to achieve sustainability: A state-of-the-art review [J]. Journal of Environmental Management, 2023, 343: 118221.

[25] DYER L G, RICHMOND W R, FAWELL P D. Simulation of iron oxide/silica precipitation in the paragoethite process for the removal of iron from acidic zinc leach solutions [J]. Hydrometallurgy, 2012, 119/120: 47−54.

[26] LANGOV S, MATYSEK D. Zinc recovery from steel-making wastes by acid pressure leaching and hematite precipitation [J]. Hydrometallurgy, 2010, 101(3): 171−173.

[27] HUANG Yu-kun, GUO Hao-jie, ZHANG Chen, LIU Bi-he, SONG Xiang-yu, ZHU Xiao-feng. A novel method for the separation of zinc and cobalt from hazardous zinc−cobalt slag via an alkaline glycine solution [J]. Separation and Purification Technology, 2021, 273: 119009.
[28] JIA Li-juan, ZHONG Ying-ying, LI Kai, LI Bin, LIU Tian-cheng, WU Wang-qin, FENG Jia-yue. Recovery of zinc resources from secondary zinc oxide via composite ammonia leaching: Analysis of Zn leaching behavior [J]. Chemical Engineering Journal, 2023, 472: 144930.
[29] HOLLOWAY P C, ETSELL T H, MURLAND A L. Use of secondary additives to control the dissolution of iron during Na_2CO_3 roasting of La oroya zinc ferrite [J]. Metallurgical and Materials Transactions B, 2007, 38(5): 793−808.
[30] LI Mi, PENG Bing, CHAI Li-yuan, PENG Ning, YAN Huan, HOU Dong-ke. Recovery of iron from zinc leaching residue by selective reduction roasting with carbon [J]. Journal of Hazardous Materials, 2012, 237: 323−330.
[31] YAN Huan, CHAI Li-yuan, PENG Bing, LI Mi, HOU Dong-ke. Reduction roasting of high iron-bearing zinc calcine under a CO−CO_2 gas: An investigation of the chemical and mineralogical transformations [J]. JOM, 2013, 65(11): 1589−1596.
[32] LI Chen, LIU Wei, JIAO Fen, YANG Cong-ren, LIU Shi-yang, QIN Wen-qing. Separation and recovery of zinc, lead and iron from electric arc furnace dust by low temperature smelting [J]. Separation and Purification Technology, 2023, 312: 123355.
[33] YAN Huan, CHAI Li-yuan, PENG Bing, LI Mi, PENG Ning, HOU Dong-ke. A novel method to recover zinc and iron from zinc leaching residue [J]. Minerals Engineering, 2014, 55: 103−110.
[34] HAN Jun-wei, LIU Wei, QIN Wen-qing, JIAO Fen, LAING Chao. Thermodynamic and kinetic studies for intensifying selective decomposition of zinc ferrite [J]. JOM, 2016, 68(9): 2543−2550.
[35] CHEN Shao-qin, ZENG Xiang-fei, LIANG Qian, HU Ling, WANG Rong. Zinc efficiently extracted from zinc calcine by reduced wet grinding: $ZnFe_2O_4$ to ZnO and Fe_3O_4 [J]. Journal of Cleaner Production, 2023, 399: 136536.
[36] ZHANG Han-quan, ZHANG Peng-fei, ZHOU Feng. Application of multi-stage dynamic magnetizing roasting technology on the utilization of cryptocrystalline oolitic hematite: A review [J]. International Journal of Mining Science and Technology, 2022, 32: 865−876.
[37] WANG Yun-yan, ZHANG Li-min, PENG Ning, YAN Xu, LIANG Yan-jie, JIANG Guo-min. Formation mechanism of zinc ferrite in high-temperature roasting of zinc oxide and ferric oxide [J]. Journal of Analytical and Applied Pyrolysis, 2020, 149: 104832.
[38] KASHYAP V, TAYLOR P. Selective extraction of zinc from zinc ferrite [J]. Mining, Metallurgy & Exploration, 2021, 38: 27−36.
[39] WU C C, CHANG F C, CHEN W S, TSAI M S, WANG Y N. Reduction behavior of zinc ferrite in EAF-dust recycling with CO gas as a reducing agent [J]. Journal of Environmental Management, 2014, 143: 208−213.
[40] YU Gang, PENG Ning, ZHOU Lan, LIANG Yan-jie, PENG Bing, CHAI Li-yuan. Selective reduction process of zinc ferrite and its application in treatment of zinc leaching residues [J]. Transactions of Nonferrous Metals Society of China, 2015, 25(8): 2744−2752.

采用还原−磁化焙烧法从高铁锌焙砂中选择性浸出锌

张添富，韩俊伟，刘 森，刘 维，李 琛，焦 芬，覃文庆

中南大学 资源加工与生物工程学院，长沙 410083

摘 要：为实现高铁锌焙砂中锌的选择性浸出，提出一种将还原焙烧与磁化焙烧相结合以强化铁酸锌选择性分解的新工艺。通过热力学分析和焙烧实验，详细研究铁酸锌的分解机理。结果表明，在 8% CO(体积分数)、750 ℃、50% CO/(CO+CO_2)(体积分数)和 90 min 的最佳还原焙烧条件下，锌焙砂中 94.65%的铁酸锌被还原分解为氧化锌和氧化亚铁。随后，还原焙砂在 450 ℃的空气气氛中磁化焙烧 30 min 后，焙砂中的氧化亚铁被选择性地磁化为四氧化三铁。磁化焙砂经低酸浸出后，焙砂中 93.62%的锌被浸出进入溶液，而 90%以上的铁以磁铁矿的形式富集在浸出渣中，浸出渣中的铁可通过磁选法进一步回收。

关键词：铁酸锌；锌焙砂；还原焙烧；磁化焙烧；酸性浸出

(Edited by Wei-ping CHEN)